Extended Abstracts of the 1998 International Conference on Solid State Devices and Materials, Hiroshima, 1998, pp. 272-273

Transmission Electron Microscopic Study of $TiSi_2$ Microstructures and the C49-C54 Phase Transformation in Narrow Lines

M. Okihara, K. Tai[1], M. Kageyama[1], Y. Harada[1], N. Hirashita, and H. Onoda[1]
VLSI Research & Development Center, LSI Production Division[1], Oki Electric Industry Co., Ltd.,
Higashi-asakawa, Hachioji, Tokyo 193-8550, Japan
Phone:+81-426-62-6108, Fax:+81-426-67-8367, E-mail; okihara274@hac.oki.co.jp

1.Introduction

$TiSi_2$ is widely used for ultra-large-scale integrated (ULSI) devices because of low resistivity and high-temperature stability. In order to overcome well-known narrow line effects, a self aligned silicide (salicide) process including the pre-amorphization implantation (PAI) treatment has been performed to achieve low sheet resistance and successful implementation into a sub-micron technology[1,2]. In this work, microstructural characteristics of $TiSi_2$ with and without PAI treatment are investigated by transmission electron microscope (TEM).

2.Experimintal

Line and space patterns were fabricated on Si (001) wafers by using electron beam lithography and conventional LOCOS process. N^+ diffusion regions were formed by As^+ implantation at 50 keV with $5x10^{15}$ cm^{-2} and the subsequent activation rapid thermal annealing (RTA) at 1050 °C for 10 seconds. The PAI treatment was carried out by As^+ implantation at 40 keV with $3x10^{14}$ cm^{-2}. In this work, implantation processes were performed without cap oxide layers to prevent oxygen contamination[3]. After surface cleaning, 40 nm-thick Ti film was sputter deposited on samples with and without PAI treatment. Then 1st RTA was performed at 650 °C for 30 seconds in N_2 ambient. After the removing TiN and unreacted Ti, 2nd RTA was carried out at 825 °C for 30 seconds. The microstructural characteristics of $TiSi_2$ were examined by TEM observation with acceleration voltage 200 kV.

3.Results and Discussion

Figures 1(a) and (b) show bright-field planar TEM images of the C49 structures after the 1st RTA in 0.94 μm line pattern with and without PAI treatment, respectively. The PAI treatment provides smaller grain size and heavily defective C49 structures. The C54 structures after the 2nd RTA are also shown in Fig. 2(a) and (b). The average grain sizes in both of C49 and C54 structures are summarized in table I. If each C54 grain can be considered to grow from one nucleation site, quite a few nucleation sites exist for both with and without PAI treatments. The C54 phase is considered to occur predominantly at triple points of the C49 grain boundaries[4]. However, Saenger et al. pointed out that all triple-points do not act as C54 nucleation site[5], suggesting that other dominant factors which cause the phase transformation must exist.

In order to examine the dominant factors for the phase transformation, microstructures of C49-$TiSi_2$ with PAI treatment are investigated in detail. Typical defect distributions are frequently observed in the 0.94 μm line-pattern sample, as shown in Fig. 3. It is noticed that defects are continuously introduced to adjoining C49 grains with slightly tilting and finally formed with striation-like distribution. However, such ordered defects hardly observed at the center region, as circled in Fig. 3.

Figures 4(a) and (b) show selected area diffraction (SAD) patterns obtained from the center (less-defective region) and the outside region (circularly defective region), respectively. Although many C49 grains are included in the selected areas, these SAD patterns are high 6-hold-rotation symmetry. It indicates that C49 grains are well ordered with same orientation. It is also noticed that all diffraction spots in Fig. 4(b) become streaky form. Since diffraction spots tend to streak to the normal direction for the defects, the defects are classified as stacking fault[6]. These results suggest two-dimensional growth of C49 grains from the less-defective regions toward the outside regions. The circular defects are presumably introduced to relieve local stress which is induced outside regions by lattice mismatches at small angle tilt grain boundaries.

Furthermore, quite large grains that are identified with C54 phase are occasionally observed in the vicinity of circular distributed defects, as shown in Fig. 5. It indicates that the phase transformation already occurs in spite of lower temperature range. In Fig. 5, the less-defective region is denoted by the circle. C54 grains exist at circularly defective regions rather than less-defective regions. It suggests that preferential nucleation sites for the C54 phase are contained in the defective regions. In this regions, residual local stress is supposed to be remained even after the defects formation or induced at boundaries between the two-dimensional growth group and other growth groups of C49-$TiSi_2$. It is considered to reduce a free-energy barrier for the nucleation of the C54 phase.

4.Conclusions

Microstructural characteristics of C49-$TiSi_2$ with and without PAI treatment are investigated from TEM observations. The circularly distributed defects are observed around less-defective regions in the C49-$TiSi_2$ with the PAI treatment. C49 grains indicate high 6-hold-rotation symmetry in not only less-defective regions but also circularly defective regions. It indicates two-dimensional growth of C49 grains. Moreover, C54 grains are already formed near the circularly defects regions. The residual local stress in the circularly defective regions is presumed to reduce the free-energy barrier for the C54 nucleation and promote the phase transformation.

References

1) I. Sakai et al., VLSI Tech. Dig. 66 (1992).
2) J. A.Kittl et al., Symp. VLSI Tech. Dig. 14 (1996).
3) H. Kotaki et al., Jpn. J. Appl. Phys., **33**, 532 (1994).
4) Z. Ma et al., J. Appl. Phys. **77**, 4384 (1995).
5) K. L. Saenger et al., J. Appl. Phys. **78,** 7040 (1995).
6) P.B. Hirsch et al., *Electron Microscopy of Thin Crystals*, Butterworths, p. 107 (1977).

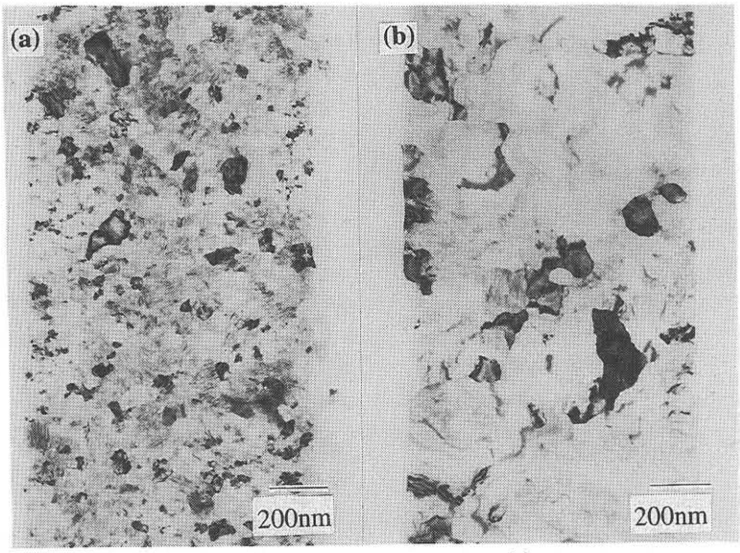

with PAI *without PAI*

Fig. 1 Planar TEM images of the C49 structures in 0.94 μm line pattern

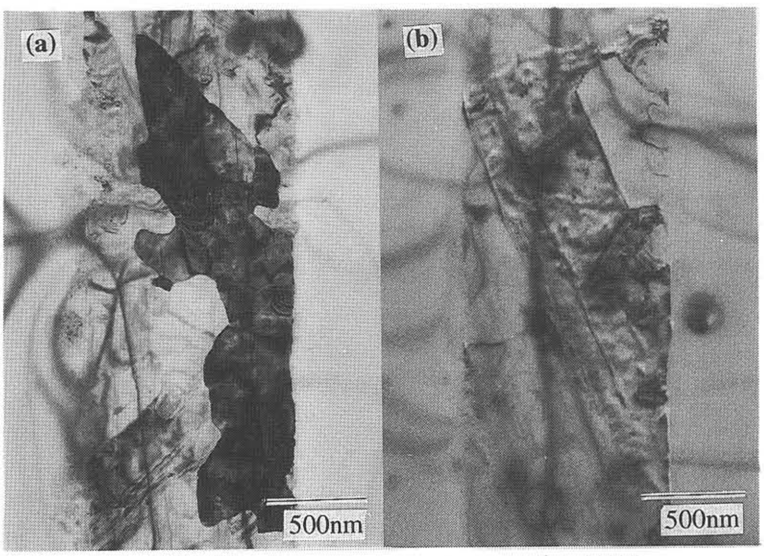

with PAI *without PAI*

Fig. 2 Planar TEM images of the C54 structures in 0.94 μm line pattern

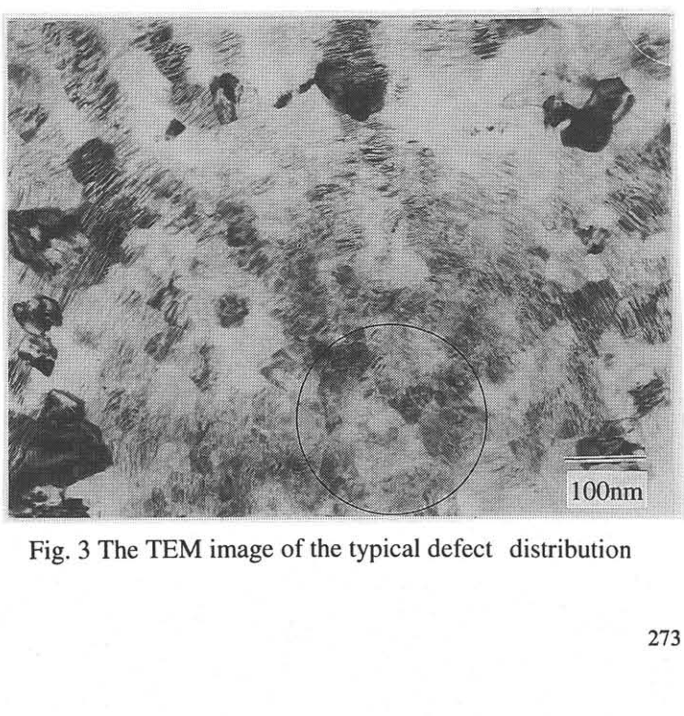

Fig. 3 The TEM image of the typical defect distribution

Table I. Average grain sizes

	with PAI	without PAI
C49	0.055μm	0.21μm
C54	~1.0μm	>10μm (with sub-grain boundaries)

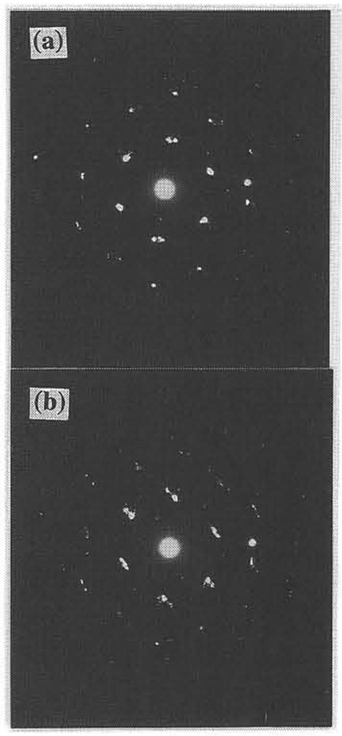

Fig. 4 SAD patterns obtained from (a) the less-defective and (b) the outside circularly defective regions

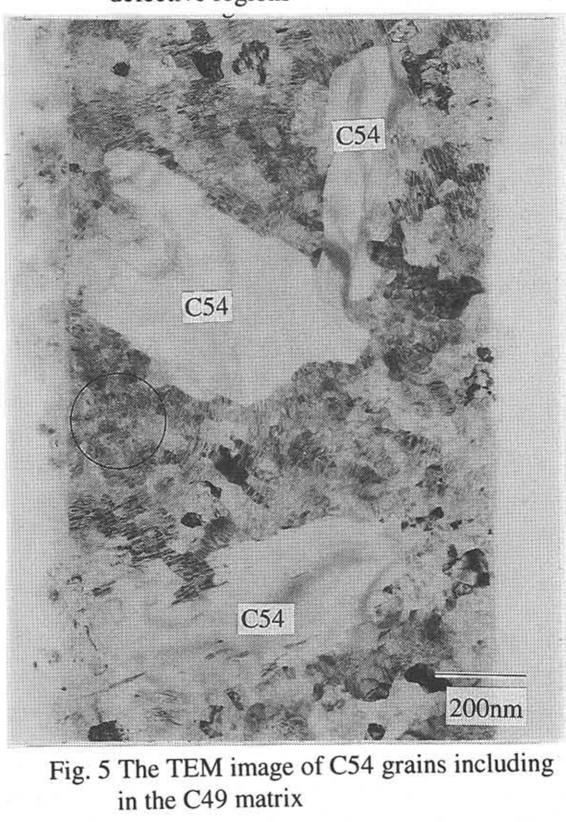

Fig. 5 The TEM image of C54 grains including in the C49 matrix